

## SIMULATION OF PIANO SUSTAIN-PEDAL EFFECT BY PARALLEL SECOND-ORDER FILTERS

*Stefano Zambon*

Dept. of Computer Science,  
University of Verona  
Verona, Italy  
stefano.zambon@univr.it

*Heidi-Maria Lehtonen*

Dept. of Signal Processing and Acoustics,  
Helsinki University of Technology, TKK  
Espoo, Finland  
heidi-maria.lehtonen@tkk.fi

*Balázs Bank*

Dept. of Computer Science,  
University of Verona  
Verona, Italy  
bank@mit.bme.hu

### ABSTRACT

This paper presents a sustain-pedal effect simulation algorithm for piano synthesis, by using parallel second-order filters. A robust two-step filter design procedure, based on frequency-zooming ARMA modeling and least squares fit, is applied to calibrate the algorithm from impulse responses of the soundboard and the string register. The model takes into account the differences in coupling between the various strings. The algorithm can be applied to both sample-based and physics-based piano synthesizers.

### 1. INTRODUCTION

The sustain pedal is an essential feature of the piano. When the sustain pedal is pressed down, the dampers lying on the strings are lifted in order to let the string register vibrate freely. Recently, Lehtonen et al. [1] showed that the sustain pedal affects the tone by increasing the decay rates of the partials, especially in the middle range of the piano. In addition, the amplitude beating characteristics are changed and the energy of the residual signal is increased compared to the tones that are played without the sustain pedal. Sympathetic string resonance has been studied from a theoretical point of view by Le Carrou et al. [2], who have constructed an analytical model of a generic string instrument.

The effect of the sustain pedal needs to be taken into account in high-quality sound synthesis. Different methods for modeling the sustain-pedal effect can be found in the literature. De Poli et al. [3] presented a sustain-pedal synthesis algorithm that is based on the simulation of 18 lowest strings of the piano plus 10 strings of variable-length, which together simulate the resonating string register. Recently, Lehtonen et al. [1] presented a model, which basically is a reverberation algorithm that consists of 12 simplified string models corresponding to the lowest tones of the piano. For physics-based piano synthesizers, a common approach [4, 5, 6, 7] is to use a separate set of string models to simulate sympathetic resonances. Borin et al. [8] suggested a physics-based method where the different string models are coupled to a common bridge admittance filter. Van Duyne and Smith [9] proposed that the effect of the sustain pedal can be taken into account by using commuted

synthesis; the impulse response of the system consisting of the soundboard and open strings is commuted to the excitation point. The drawback of this method is that it cannot be applied to other synthesis paradigms.

This paper presents a model for simulating the sustain-pedal effect with a set of resonators, which can be considered as string models that are used for creating sympathetic resonance. The advantage over previous methods is found in the parameterization procedure that allows the direct calibration starting from measured impulse responses. On the other hand, the computational cost is higher compared to the other methods. Nevertheless, a real-time implementation is affordable using current entry-level computer hardware.

The paper is organized as follows: First, in Sec. 2 the model structure is presented. Section 3 discusses the model calibration based on the soundboard and string register impulse response measurements. Section 4 discusses some extensions of the model and Sec. 5 presents results obtained with the proposed algorithm. Finally, Sec. 6 concludes the paper.

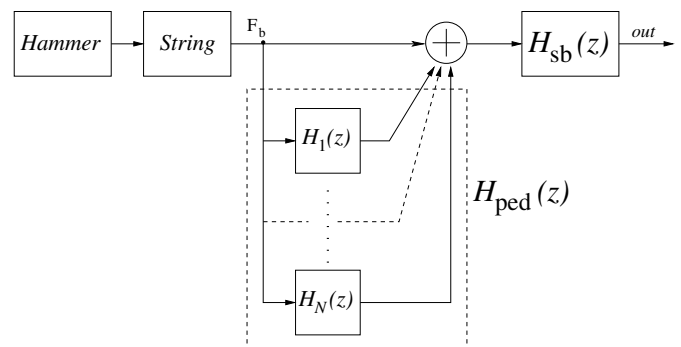


Figure 1: Block diagram for sustain pedal simulation through a parallel filter bank  $H_{ped}$ , here inserted in a typical scheme for physics-based piano synthesis.

## 2. SYNTHESIS MODEL

The architecture of the proposed synthesis algorithm is depicted in Fig. 1, when sustain pedal simulation is added to a typical scheme for physics-based piano sound synthesis [10, 11]. The modeling blocks resemble the functional parts of a real piano. The signal coming from the hammer simulation block is the excitation for the string resonator, which is a linear filter with a set of quasi-harmonic resonances. The output of the string model is the transversal force at the bridge  $F_b$ . This is fed into the sympathetic string register  $H_{\text{ped}}$  and, through a separate parallel path, to the soundboard radiation filter  $H_{\text{sb}}$ . It has to be noticed that, in the real piano, all the strings and the instrument body are coupled together, so the bidirectional coupling between the different modeling blocks should be considered in a proper physical model. However, the main effects of the body termination can be taken in account by changing the partial frequencies and decay times of the string model [10] thus permitting a feed-forward model for the instrument body and the sympathetic string register.

Due to the linear and time invariant nature of the sympathetic string register block  $H_{\text{ped}}(z)$  and the soundboard filter  $H_{\text{sb}}(z)$ , the proposed algorithm can be applied also to other synthesis paradigms, such as commuted synthesis [9] or sampling synthesis. In these cases, the pedal is implemented as a post-processing stage: the “dry” piano sound is filtered by  $H_{\text{ped}}(z)$  and the processed signal is added to the original, corresponding to a filtering with  $H_{\text{ped}}(z) + 1$ .

From the signal processing point of view, the transfer function of the block for the sustain pedal simulation is a parallel connection of  $K$  second-order resonators,

$$H_{\text{ped}}(z) = \sum_{k=1}^K H_k(z), \quad (1)$$

where each one of the transfer functions  $H_k(z)$  can be described as two parallel complex resonators,

$$H_k = \frac{c_k}{1 - p_k z^{-1}} + \frac{c_k^*}{1 - p_k^* z^{-1}} = \frac{b_{k,0} + b_{k,1} z^{-1}}{1 + a_{k,1} z^{-1} + a_{k,2} z^{-2}}. \quad (2)$$

In Eq. (2),  $p_k, p_k^*$  are the conjugate poles,  $c_k, c_k^*$  are the complex amplitudes of the resonators and  $b_k, a_k$  are the numerator and denominator coefficients of the real valued second-order section.

The physical justification behind Eq. (1) comes from the fact that the sympathetic string register presents a linear behaviour [1] and its motion can therefore be decomposed into a set of normal modes which are simulated by the discrete resonators  $H_k(z)$ . However, implementing all the modes interacting in the real sympathetic register would be prohibitive even with currently available hardware. It is thus necessary to choose a subset of significant modes which are perceptually relevant for sustain pedal simulation.

## 3. MODEL CALIBRATION

Here, we address the problem of calibrating the parallel second-order filter bank in order to approximate the measured impulse response. The target system shows a complex behaviour due to the high number of modes and the coupling with the soundboard. For

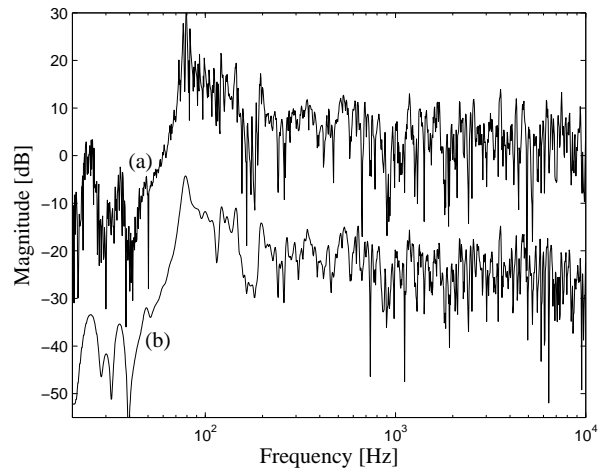


Figure 2: Example magnitude transfer function of (a) the soundboard plus the string register  $\|\tilde{H}_{\text{ped}}(z)\|$  and (b) the soundboard alone  $\|H_{\text{sb}}(z)\|$ . The sharp peaks corresponding to string resonances can easily be noticed in (a), especially in the low frequency range. The curves are offset for clarity.

this reason, a robust two-step procedure is used. First, the poles of the system are found using a spectral zooming technique [12, 13]. The pole set found in this way is reduced with simple heuristics. Then, a least-square fit [14, 15] is used to find the complex amplitudes of the resonators (i.e., the zeros of the system).

The impulse response of the soundboard  $h_{\text{sb}}$  can be obtained by hitting the bridge with an impact hammer, measuring simultaneously the hammer force and the sound pressure in a given position. Then, the impulse response is computed by deconvolution of the two signals. The impulse response with the freely vibrating strings  $\tilde{h}_{\text{ped}}$  is obtained in an analogous way. Fig. 2 illustrates some examples of the transfer functions obtained with this procedure.

As can be seen in the block diagram of Fig. 1, the relation between the measured transfer function  $\tilde{H}_{\text{ped}}$  and the transfer function of the parallel bank  $H_{\text{ped}}$  can be expressed as

$$\tilde{H}_{\text{ped}} = H_{\text{sb}} + H_{\text{sb}} \cdot H_{\text{ped}}. \quad (3)$$

Accordingly, the system identification problem can be formulated

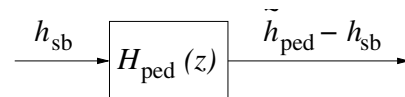


Figure 3: Identification of the target system  $H_{\text{ped}}(z)$  using the measured impulse responses as input and output.

as estimating the system which produces the output  $\tilde{h}_{\text{ped}} - h_{\text{sb}}$  when the signal  $h_{\text{sb}}$  is given as an input, as it is shown in Fig. 3. The required target output response of the model is  $h_t = \tilde{h}_{\text{ped}} - h_{\text{sb}}$ .

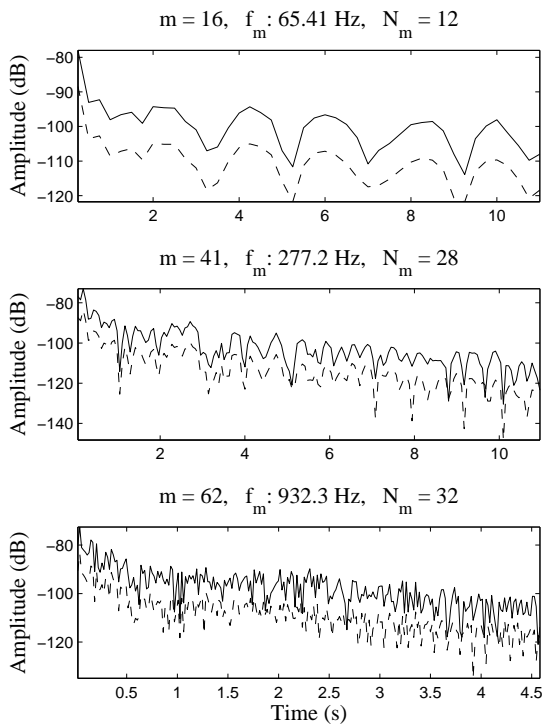


Figure 4: Examples of system identification with FZ-ARMA modeling for some subbands. In the pictures, the target decimated signal (solid line) is plotted over the response of the modeled system (dashed line).  $N_m$  stands for the number of poles used for the estimation. The curves are offset for clarity.

### 3.1. Pole estimation

The first step in the estimation procedure is finding the prominent poles of the target system. This task is solved by the means of frequency-zooming ARMA (FZ-ARMA) analysis, a spectral zooming technique that has been shown to work well for resolving very closely positioned modes and high-density modal clusters [12, 13]. The basic idea of FZ-ARMA method is to divide the frequency spectrum in subbands and apply standard ARMA modeling techniques to estimate the poles and the zeros in each subband. The method is well suited for the analysis of the string register, because to a good approximation the frequencies of the modes are close to the frequency distribution given by the equal temperament. In other words, since we know a theoretical distribution for the frequencies of the signal, we can use these as center frequencies for our analysis procedure. As an example, around 523.251 Hz, corresponding to the note C5, we should expect to find all the modes relative to the fundamental of C5, the ones relative to the second partial of C4 (which has the fundamental at  $523.251/2=261.626$  Hz), the third partial of F3 (fundamental  $523.25/3=174.614$ Hz) and so on.

We thus divide the spectrum in  $N_b$  non-overlapping subbands, having center frequencies at

$$f_m = 440 \cdot 2^{(m-49)/12} \quad (4)$$

and bandwidths

$$BW_m = 2 \left( \sqrt{2^{1/12}} - 1 \right) f_m, 1 \leq m \leq N_b. \quad (5)$$

The integer index  $m$  corresponds, for the first 88 values, to the key index on the piano keyboard (the 49th piano key is A4 at 440Hz).  $N_b = 104$  bands were used, corresponding to a highest frequency analysis of 10548 Hz. For each subband  $m$  the following steps are executed:

1. The target response  $h_t(n) = \tilde{h}_{ped}(n) - h_{sb}(n)$  is modulated to DC by multiplication with the complex signal  $e^{j2\pi f_m n / f_s}$ , where  $f_s$  is the original sampling frequency.
2. Lowpass filtering and decimating up to  $f_{s,m}$  is applied to the resulting signal. The new sampling frequency  $f_{s,m}$  equals the current bandwidth  $BW_m$  as computed from Eq. (5).
3. Steiglitz-McBride iteration is used to find the zeros and poles of the decimated signal. The number  $N_m$  of the poles depends on the subband, and it is set to  $N_m = 2$  for the lowest bands and linearly increases up to  $N_m = 32$  for the 45th band. This is because the modal density increases with the frequency but, at the same time, we should also impose an upper limit for the filter order motivated by implementation constraints and by the logarithmic frequency resolution of the hearing. The number of zeros in each subband is set to  $N_m/2$ . Note that the zeros are not used in the later steps of the calibration.
4. The poles from ARMA analysis are mapped to the full sample rate by counter-rotating the phase of a factor  $2\pi f_m / f_s$  and by scaling their radii to compensate the decimation process.

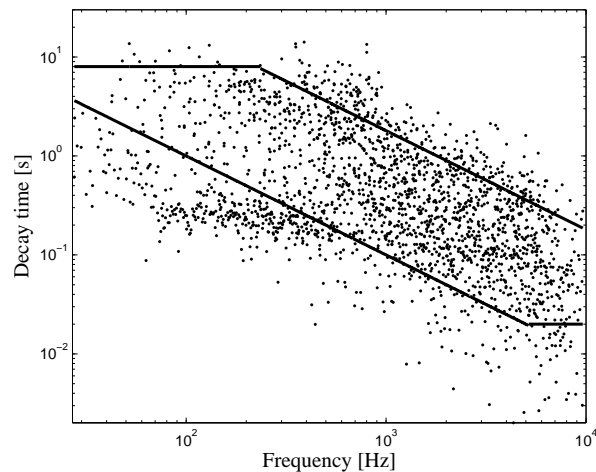


Figure 5: Modal distribution obtained with FZ-ARMA analysis and heuristic limits to remove noisy or fast decaying modes.

The accuracy of the results with FZ-ARMA analysis depends on the right choice of parameters in relation to the target signal. Better estimates are achieved by taking different portions of the original signal depending on the band. In this way the ratio between free parameters and available data (i.e., the length of the subsampled signal) does not vary much between different bands.

Skipping the first part of the subsampled signal also helped the estimate in the mid-high frequency range, where the procedure tends to overdamp the system poles. This also facilitates to minimize the influence of the transients coming from the interpolation filters used for decimation. Fig. 4 presents some examples of modeling with this technique.

The outcome of the FZ-ARMA analysis procedure consists in a large set of poles (around 2500 in our case). This set is processed with simple heuristics in order to discard estimation errors (such as unstable poles) and, possibly, reduce it to a subset of perceptually relevant poles. In our case, for example, we discarded the poles which were close to their band's boundaries and those which have very short or too long decay times. Fast decaying modes are eliminated because their decay times are in the same magnitude order of those of the soundboard, and their perceptual effect is masked by modes with longer decay times. However, modes with too long a decay time probably correspond to modeling measurement noise. Fig. 5 shows the distribution of decay times versus frequency and the limits imposed with the heuristics. These limits are defined on an empirical base and try to follow the main trend of modes distribution. In particular, the sloped lines correspond to imposing a  $1/f$  limit on the decay times  $\tau_k$ :

$$\frac{T_{min}}{f_k} \leq \tau_k \leq \frac{T_{max}}{f_k}. \quad (6)$$

Finally, the denominator coefficients  $a_{k,1}$  and  $a_{k,2}$  of 2 are directly determined by the poles  $p_k$ . As a further optimization, the number of second-order sections applied in the model can be reduced by taking into account the masking effect of neighbouring resonances.

### 3.2. Least squares fit to measured response

Now the feedforward coefficients  $b_{k,0}$  and  $b_{k,1}$  have to be estimated. This is a linear-in-parameter system identification problem and the estimation is done similarly as in [15].

Let us denote  $u_k$  the impulse response of the system  $1/(1 + a_{k,1}z^{-1} + a_{k,2}z^{-2})$ , which is the denominator part of  $H_k(z)$  as in Eq. (2). Then, the output of the system can be written as follows:

$$h(n) = h_{ped}(n) * h_{sb}(n) = \sum_{k=1}^K b_{k,0} u_k(n) * h_{sb} + b_{k,1} u_k(n-1) * h_{sb} = \sum_{k=1}^K b_{k,0} s_k(n) + b_{k,1} s_k(n-1), \quad (7)$$

where  $*$  denotes convolution. The signal  $s_k(n) = u_k(n) * h_{sb}(k)$  is the soundboard response  $h_{sb}(n)$  filtered by  $1/(1 + a_{k,1}z^{-1} + a_{k,2}z^{-2})$ . It can be seen that Eq. (7) is linear in its free parameters  $b_{k,0}$  and  $b_{k,1}$ . Writing Eq. (7) in matrix form yields

$$\mathbf{h} = \mathbf{M}\mathbf{p}, \quad (8)$$

where  $\mathbf{p} = [b_{1,0}, b_{1,1}, \dots, b_{K,0}, b_{K,1}]^T$  is a column vector composed of the free parameters. The rows of the modeling signal matrix  $\mathbf{M}$  contain the modeling signals, which are  $s_k(n)$  and their delayed counterparts  $s_k(n-1)$ . Finally,  $\mathbf{h} = [h(0) \dots h(N)]^T$  is a column vector composed of the resulting response.

The problem reduces to finding the optimal parameters  $\mathbf{p}_{opt}$  such that  $\mathbf{h} = \mathbf{M}\mathbf{p}_{opt}$  is closest to the target response  $\mathbf{h}_t =$

$[h_t(0) \dots h_t(N)]^T$ , where  $h_t = \tilde{h}_{ped} - h_{sb}$ . If the error function is evaluated in the mean squares sense, the optimum is found by the well known LS solution

$$\mathbf{p}_{opt} = (\mathbf{M}^H \mathbf{M})^{-1} \mathbf{M}^H \mathbf{h}_t, \quad (9)$$

where  $\mathbf{M}^H$  is the conjugate transpose of  $\mathbf{M}$ .

It may be not practical to compute all the parameters at the same time, because of the high order of the matrix  $\mathbf{M}$ . However, the different modeling signals are almost orthogonal because they can be thought as slowly decaying sinusoids having different frequencies. It is thus possible to solve Eq. (9) separately for each subband, with significant savings in the overall computation time.

### 3.3. Physically informed model calibration

The calibration method proposed above can only be applied if the appropriate impulse responses are available. Otherwise, a possible alternative to obtain the poles and amplitudes of each resonator comes from modal synthesis of the piano string [16], i.e., from the discretization of the modal solution of the string equation. For each key, a limited set of a few (4–32) resonators corresponding to the first partials of the string is chosen. This choice leads to a total number of 700–1200 resonators up to 10 kHz, which should be enough in any case since the sustain-pedal effect is relevant only in the low and middle frequency range [1]. This kind of an approach is particularly convenient in the case of a physics-based piano model where a secondary bank of resonators is already present, for example when it is used for the simulation of beatings and two-stage decay [10]. Similar techniques for sympathetic resonance simulation were already used in literature, e.g. [4, 5, 6]. The obvious drawback of this calibration method is that it is not based on the measurement of real string resonance responses, and it generally needs manual tuning to produce good results.

## 4. DISCUSSION

The synthesis method proposed, together with the calibration method, is already sufficient to provide an accurate simulation of the sustain pedal effect. Here, some issues regarding the inclusion of the algorithm in a complete piano synthesizer are discussed. First, an extension is provided to vary the effect for the different strings. Then, an estimation of the overall computational cost is given.

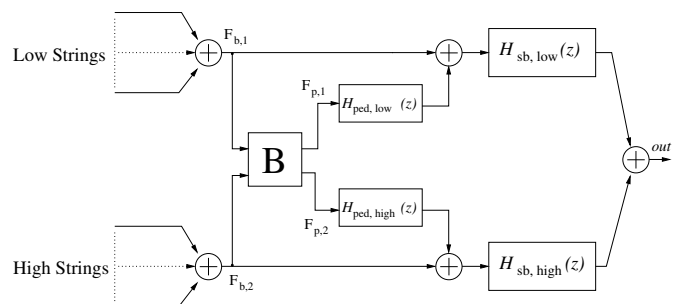


Figure 6: Example of string subdivision in two different groups. The gain matrix  $\mathbf{B}$  controls the energy exchange between the string groups.

#### 4.1. Variation of the effect for the different strings

In the synthesis structure of Fig. 1 the effect is the same for all the piano keys. This is in contrast to what happens in the real piano, where the string register is excited differently by various strings. We propose to partially solve this issue by splitting the keyboard in  $R$  different regions and using different pedal and soundboard model for each region. A similar approach for applying different soundboard filters has already been used in literature [17].

In Fig. 6 the situation is depicted for the case  $R = 2$ . The relationship between the cumulated output of the string models  $\mathbf{F}_b = [F_{b,0}, \dots, F_{b,R}]$  and the inputs  $\mathbf{F}_p = [F_{p,0}, \dots, F_{p,R}]$  of the parallel banks is controlled by a  $R \times R$  gain matrix  $\mathbf{B}$ :

$$\mathbf{F}_p = \mathbf{B} \mathbf{F}_b. \quad (10)$$

By selectively damping a set of strings, one can obtain the impulse responses needed to calibrate the separated resonator banks of Fig. 6. This should also provide better estimates because the number of modes is lower. It is an open question how to accurately estimate the parameters of the matrix  $\mathbf{B}$ . However, the parameters are easily controllable and manual tuning is possible.

One further advantage of this approach is that different string groups are filtered by different soundboard responses, which are implemented as separate filters in the most straightforward way. However, depending on the particular implementation of the soundboard radiation filters, some optimizations can be used to reduce the computational complexity, since the different soundboard models share a common set of resonances [14, 17].

#### 4.2. Computational cost

A practical number for the order  $R$  of the matrix  $\mathbf{B}$  is in the range 2–8. Consequently, the computational cost is dominated by the update of the  $K$  resonators, which require 4 multiply-and-add operations each if implemented with a one-zero, two-pole real valued IIR filter. Since  $K$  is typically in the order of 1000, the cost is remarkably higher if compared to the efficient reverb-based models already presented in literature [1, 3]. However, the computational complexity can be significantly reduced if the pedal model is implemented as a multirate algorithm. The upsampling and downsampling filters can be of low order, since their passband errors can be easily corrected by changing the amplitudes and phases of the second-order resonators, similarly as done in [18] for modeling beating and two-stage decay. Moreover, the structure is highly vectorizable and thus it can exploit the SIMD constructs found in modern DSPs and general purpose CPUs.

### 5. EXPERIMENTS

The proposed calibration algorithm has been tested on impulse responses taken from a Steinway grand piano Model C. The measurements were done in a recording studio, placing the microphones 2m away from the soundboard, and hitting the bridge by an impulse hammer. The magnitudes of the measured transfer functions can be observed in Fig. 2. A parallel bank of  $K = 1500$  second-order sections has been designed by the FZ-ARMA and least squares method proposed in Sec. 3. In order to validate the analysis process, the recorded signal  $y(n)$  has been resynthesized by convolving the recorded impulse hammer force with the im-

pulse response of the designed parallel bank<sup>1</sup>. The expression for the resynthesized signal  $y_r(n)$  is thus

$$y_r(n) = F_h(n) * (h_{ped}(n) * h_{sb}(n) + h_{sb}(n)) \quad (11)$$

where  $F_h(n)$  is the recorded hammer force. Fig. 7 compares the time-frequency behaviour of the original and the resynthesized signals  $y(n)$ ,  $y_r(n)$ . Due to the intrinsic limits of the analysis procedure, some differences can be noticed in the middle and high frequency range. The source of these errors is found in the accuracy of the FZ-ARMA analysis, which can be improved by tweaking the parameters and heuristics used. However, the lack of some particular resonances is not a problem, since the result still can be recognized as the sustain pedal effect, and small differences are masked.

Due to practical reasons during the measurement session, only the response of the whole string register has been analyzed. The authors plan to make another set of measurements to calibrate the model for the different string groups.

The parallel bank has also been tested by applying the sustain pedal effect to dry recorded piano samples. In addition, the algorithm, including subdivision in  $R = 8$  keyboard regions, has been implemented as part of a real-time physics-based piano synthesizer developed at the University of Verona.

### 6. CONCLUSIONS

A novel method for the simulation of the piano sustain-pedal effect has been presented. Compared to previous works, our method allows a precise calibration from measured impulse responses. This is particularly useful when the purpose is to simulate the pedal effect of a given piano, which can be very advantageous when using in combination with sampling synthesis. Nevertheless, the method can be applied to other synthesis paradigms, such as physics-based modeling. An extension to the basic model has also been proposed that includes the differences in coupling of the various string groups.

Possible future work includes perceptual studies to validate the sound quality of the method and, eventually, to reduce the number of second-order sections required for the simulation. Another open issue is the modeling of other aspects of the sustain-pedal, such as half-pedaling, which is important in jazz and pop music piano playing, and the noise sounds generated by the pedal mechanism. Inclusion of these aspects should lead to a higher fidelity in the interaction with virtual piano instruments.

### 7. ACKNOWLEDGMENTS

This work was partially supported by the *Joint Project* “Sound Synthesis by Physical Models of the Piano” coordinated between the University of Verona and Viscount International SpA (2007–2008). The work of Heidi-Maria Lehtonen is supported by the GETA Graduate School, the Academy of Finland (project no. 122815), the Finnish Cultural Foundation, the Nokia Foundation, and Emil Aaltonen Foundation. The authors are thankful to Federico Fontana for his suggestions.

<sup>1</sup>Sound examples are available for listening at: <http://www.acoustics.hut.fi/go/dafx08-pedal/>

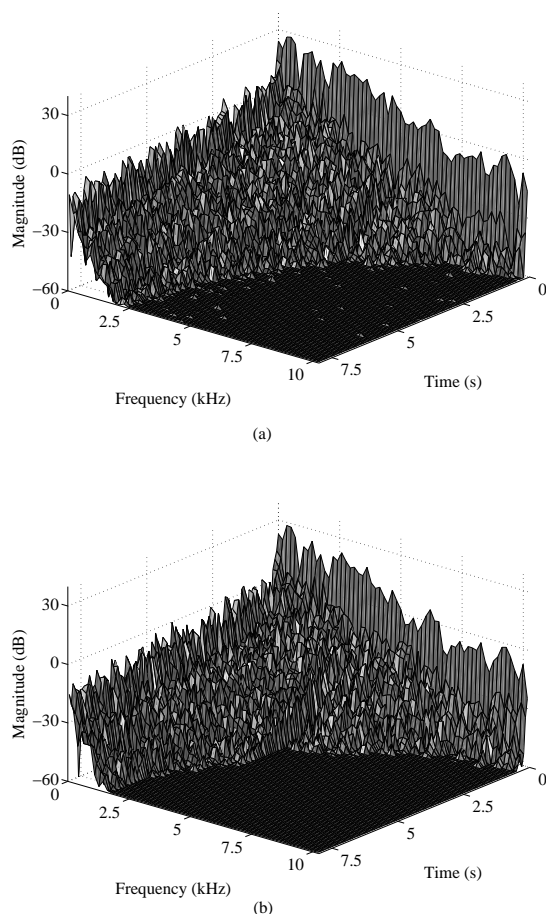


Figure 7: Time-frequency plot of (a) the recorded soundboard and string register response signal  $y(n)$  and (b) the resynthesized signal  $y_r(n)$  using the designed parallel bank.

## 8. REFERENCES

[1] H. M. Lehtonen, H. Penttinen, J. Rauhala, and V. Välimäki, "Analysis and modeling of piano sustain-pedal effects," *Journal of the Acoustical Society of America*, vol. 122, pp. 1787, 2007.

[2] J. L. L. Carrou, F. Gautier, N. Dauchez, and J. Gilbert, "Modelling of Sympathetic String Vibrations," *Acta Acustica united with Acustica*, vol. 91, no. 2, pp. 277–288, 2005.

[3] G. De Poli, F. Campetella, and G. Borin, "Pedal resonance effect simulation device for digital pianos," 1998, US Patent 5,744,743.

[4] D. A. Jaffe and J. O. Smith, "Extensions of the Karplus-Strong Plucked-String Algorithm," *Computer Music Journal*, vol. 7, no. 2, pp. 56–69, 1983.

[5] M. Karjalainen, V. Välimäki, and T. Tolonen, "Plucked-String Models: From the Karplus-Strong Algorithm to Digi-

tal Waveguides and beyond," *Computer Music Journal*, vol. 22, no. 3, pp. 17–32, 1998.

[6] J. Rauhala, *Physics-Based Parametric Synthesis of Inharmonic Piano Tones*, Ph.D. thesis, Helsinki University of Technology, 2007.

[7] J. Rauhala, M. Laurson, V. Välimäki, H.-M. Lehtonen, and V. Norilo, "A parametric piano synthesizer," *To be published in Computer Music Journal*, vol. 32, no. 4, 2008.

[8] G. Borin, D. Rocchesso, and F. Scalcon, "A physical piano model for music performance," in *Proc. International Computer Music Conference (ICMC 1997)*, Thessaloniki, Greece, 1997, pp. 350–353.

[9] J. O. Smith and S. A. Van Duyne, "Commutated piano synthesis," in *Proceedings of the 1995 International Computer Music Conference, Banff*, 1995, pp. 319–326.

[10] B. Bank, F. Avanzini, G. Borin, G. D. Poli, F. Fontana, and D. Rocchesso, "Physically Informed Signal Processing Methods for Piano Sound Synthesis: A Research Overview," *EURASIP Journal on Applied Signal Processing*, vol. 2003, no. 10, pp. 941–952, 2003.

[11] J. Rauhala, H. M. Lehtonen, and V. Välimäki, "Toward next-generation digital keyboard instruments," *IEEE Signal Processing Magazine*, vol. 24, no. 2, pp. 12–20, 2007.

[12] M. Karjalainen, P. A. A. Esquef, P. Antsalo, A. Mäkivirta, and V. Välimäki, "Frequency-zooming ARMA modeling of resonant and reverberant systems," *Journal of the Audio Engineering Society*, vol. 50, no. 12, pp. 1012–1029, 2002.

[13] P. A. A. Esquef, "Frequency-Zooming ARMA Modeling for Analysis of Noisy String Instrument Tones," *EURASIP Journal on Applied Signal Processing*, vol. 2003, no. 10, pp. 953–967, 2003.

[14] B. Bank, "Direct design of parallel second-order filters for instrument body modeling," in *Proc. International Computer Music Conference (ICMC 2007)*, Copenhagen, Denmark, Aug. 2007, pp. 458–465.

[15] B. Bank, "Perceptually motivated audio equalization using fixed-pole parallel second-order filters," *IEEE Sign. Proc. Lett.*, vol. 15, pp. 477–480, 2008.

[16] B. Bank, *Physics-based Sound Synthesis of String Instruments Including Geometric Nonlinearities*, Ph.D. thesis, Budapest University of Technology and Economics, Hungary, Feb. 2006, URL: <http://www.mit.bme.hu/~bank/phd>.

[17] B. Bank, "Physics-based sound synthesis of the piano," M.S. thesis, Budapest University of Technology and Economics, Hungary, May 2000, Published as Report 54 of HUT Laboratory of Acoustics and Audio Signal Processing, URL: <http://www.mit.bme.hu/~bank/thesis>.

[18] B. Bank, "Accurate and efficient modeling of beating and two-stage decay for string instrument synthesis," in *Proc. MOSART Workshop on Curr. Res. Dir. in Computer Music*, Barcelona, Spain, Nov. 2001, pp. 134–137.